

Predicting of Temperature Distribution in Direct Contact Heat Transfer

Najim A. Jassim

Division of Physical Science and Research – Ministry of Science and Technology – Iraq

Abstract

An experimental and theoretical investigation of three phase direct contact heat transfer by evaporation of refrigerant drops in an immiscible liquid has been carried out. Refrigerant R12 and R134a were used for the dispersed phase, while water and brine were the immiscible continuous phase. A numerical analysis is presented to predict the temperature distribution throughout the circular test column radially and axially is achieved. Experimental measurements of the temperature distribution have been compared with the numerical results and are discussed. A comparison between the experimental and theoretical results showed acceptable agreement and applicability of the derived equations. Comparison with other related work showed similar behavior.

Keywords: temperature distribution, direct contact heat transfer.

Introduction

A general method used in direct-contact heat exchange consists of injecting drops of a volatile liquid (dispersed phase) into a column of an immiscible liquid (continuous phase) whose temperature is above the boiling point of the drops. The drops will travel up the column, evaporating into two phase bubbles. Consequently, the continuous liquid phase is cooled gradually forming a gas hydrate [1].

Most of the indirect heat exchangers are subjected to corrosion, scaling and fouling problems leading to drastic decrease in the heat transfer process with time. Scaling and fouling need continuous maintenance, changing equipment and repairing. These problems lead to extra costs. Direct contact heat transfer can be considered as one of the solutions to the above problems [2].

Direct-contact heat exchangers include boilers and condensers, spray columns, perforated plate columns, sieve and baffle tray columns, packed bed columns, cross flow columns, and bubble columns. Multiphase heat exchangers that use latent heat rather than sensible heat between immiscible fluids had been effectively used in

ocean water desalination, geothermal heat recovery, thermal energy storage systems, and solar pond technology. Crystallization of ice from brine is another application. This process is similar to a gas hydrate method for desalination [3]. Theoretical and experimental studies have been reported on the heat transfer mechanism between single liquid drops and the continuous liquid phase. Heat transfer and growth associated with a compound drop that is growing because of change of phase were included. Yet information on multi drops is rare.

The development of an accurate theoretical model for the prediction of heat transfer coefficient in multi drops evaporating in an immiscible liquid is extremely difficult. This is due to the complex nature of the phenomenon and the wide variety of factors affecting it. Among the major parameters that influence this process are, bubble growth, rise velocity, driving force, drop geometry, presence of surface-active material, and the combination of two liquids.

A numerical solution of two dimensional, transient, two-phase laminar flow energy equation in cylindrical coordinates, with circular symmetry was solved for the temperature distribution throughout the column radially and axially.

Experimental Work

The experimental system is shown schematically in Fig.1. It consists of a test column (crystallizer), cold water supply system, dispersed phase supply system, and closed-loop vapor compression refrigerator.

The test column, is illustrated schematically in Fig.2. It consists of a cylindrical Pyrex glass column of 80 mm diameter and 1.20m long [4], in which the test fluid, water was confined. A rectangular Perspex water jacket was made concentrically around the inner cylindrical column. The jacket served as a constant - temperature water bath and also contributed to minimizing the distortion of the images of the bubbles or drops inside the test column. Sixteen calibrated sheathed type T thermocouples of the same type were distributed along the column in different positions to measure the temperature of the water axially and radial within the column.

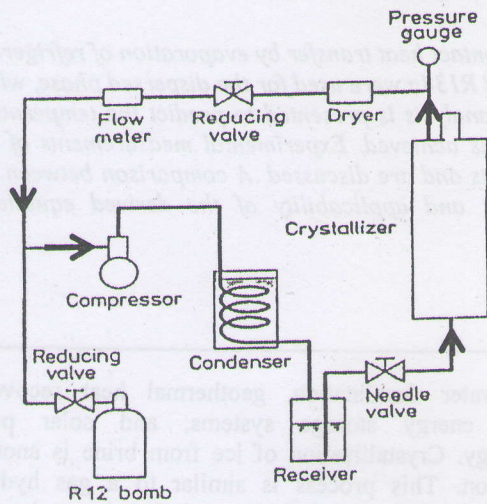


Fig.1 Schematic of experimental system

The experiments were conducted at pressure of 4 bar and by varying the following conditions: dispersed phase flow rate (0.8 to 2cc/s), temperature difference (3 to 8K), column height (0.25 to 0.5m), and brine concentration (0 to 8 wt.%). Typical experiments were conducted as follows:

1. Water was cooled in the constant temperature cooling unit to the desired temperature in the range of 15 to 20°C. Cold water from the constant temperature bath was circulated through the test column. When the water in the test column attained the desired temperature above the dispersed phase saturation temperature (12°C for refrigerant R12 and 10°C for R134a), the test column was filled with water to the desired level and the circulation was stopped.
2. The refrigerator loop was evacuated from air by the use of a vacuum pump and refrigerant was supplied from high pressure bomb to the loop till a sufficient volume of refrigerant in the liquid state was stored in the receiver.

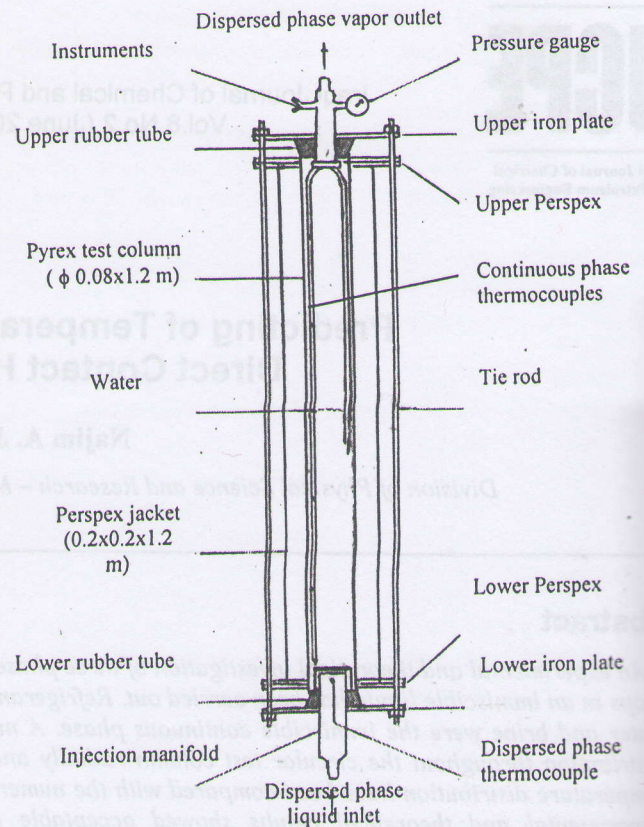


Fig.2 Assembly drawing of test column (crystallizer)

3. As the compressor began to work the refrigerant was not added from the bomb to the loop.

The needle valve was then adjusted to give the required flow rate and the required pressure of the refrigerant. Measurement of temperature and pressure in the column, as well as the flow rate of the refrigerant were immediately started. The dispersed - phase liquid drops evaporated in the stagnant water and leave the test column while the water is cooled.

Mathematical Model

Consider the upward of a bubbly flow in a vertical circular cylinder of height L and radius R_0 . A transient axial mixing flow is considered in a two dimensional cylindrical coordinate system (R, θ, Z) with axis symmetry. The governing energy equation for the continuous liquid phase is:

$$\frac{\partial T}{\partial t} + u_z \frac{\partial T}{\partial z} = \alpha \left[\frac{1}{r} \frac{\partial}{\partial r} \left(r \frac{\partial T}{\partial r} \right) + \frac{\partial^2 T}{\partial z^2} \right] - \frac{nh_d A_d}{\rho C_p V_d} (T - T_d) + \frac{\mu}{\rho C_p} \left(\frac{\partial u_z}{\partial r} \right)^2 \quad (1)$$

We introduce the following dimensionless quantities:

$$\theta = \frac{(T - T_d)}{(T_w - T_d)} \quad \text{dimensionless temperature}$$

$$\tau = \frac{u_c t}{D_o} \quad \text{dimensionless time}$$

$$R = \frac{r}{R_o}, Z = \frac{z}{D_o} \quad \text{dimensionless coordinates}$$

$$U = \frac{u_z}{u_c} \quad \text{dimensionless axial velocity}$$

$$\theta = 1 \text{ for } R = 1, 0 \leq Z \leq \frac{L}{D_o} \quad (3b)$$

$$\frac{\partial \theta}{\partial R} = 0.0 \text{ for } R = 0, 0 \leq Z \leq \frac{L}{D_o} \quad (3c)$$

Walter and Blanch [8] developed the following equation:

$$U = 1 - 6 \left(\frac{R}{R_o} \right)^2 + 5 \left(\frac{R}{R_o} \right)^3 \quad (4)$$

Sideman and Isenberg [9] developed the following equation:

$$h = 0.272 P_e^{1/2} (d/K) \quad (5)$$

and using the dimensionless groups of:

$$Pe = \frac{u_c D_o}{\alpha_3}$$

$$Re_c = \frac{u_c D_o}{\nu_3}$$

$$Pr = \frac{\mu_3 C_{p3}}{K_3}$$

$$Ec = \frac{u_c^2}{C_{p3}(T_w - T_d)}$$

$$M^2 = \frac{nh_3 d^2}{K_3 L}$$

The governing energy equation in dimensionless form becomes:

$$\frac{\partial \theta}{\partial r} + U \frac{\partial \theta}{\partial Z} = \frac{1}{Pe} \left\{ \begin{aligned} & \left[\frac{4}{R} \frac{\partial}{\partial R} \left(R \frac{\partial \theta}{\partial R} \right) + \frac{\partial^2 \theta}{\partial Z^2} \right] \\ & - M^2 \theta + 4 Ec Pr \left(\frac{\partial U}{\partial R} \right)^2 \end{aligned} \right\} \quad (2)$$

Where θ is the dependent variable; R, Z, τ are independent variables and M^2 is the heat sink term.

To solve the energy equation numerically by applying the explicit finite difference method, the derivatives in this equation could be replaced by the finite difference approximations shown in appendix A [5-7]. Equation (2) is subjected to initial and boundary conditions:

The initial condition for $\tau = 0$ is:

$$\theta = 1.0 \left(\tau = 0, 0 \leq R \leq L, 0 \leq Z \leq \frac{L}{D_o} \right) \quad (3a)$$

The boundary conditions for $\tau > 0$ are:

Results and Discussion

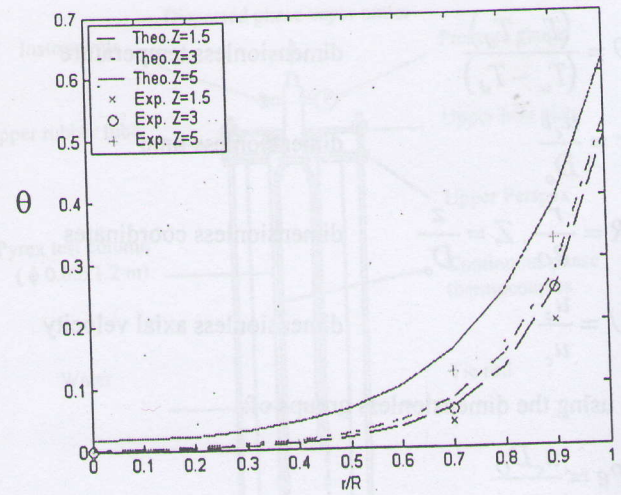
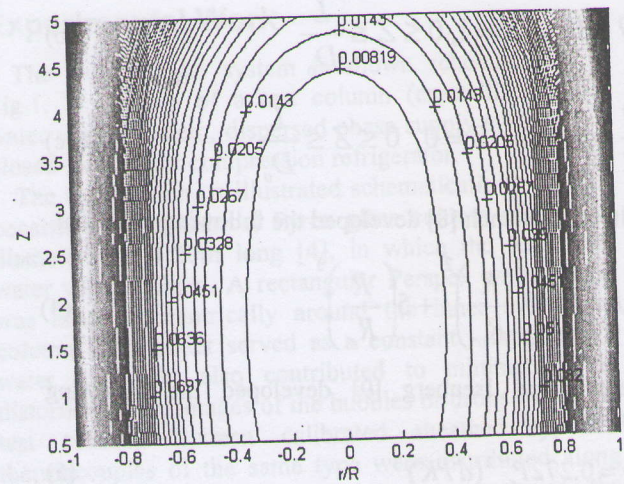
Numerical results were obtained from the computational algorithm developed in the present work. The numerical grid size was tested by using a different number of grid points in (R) and (Z) directions.

Figs. 1 to 6 show the experimental and theoretical isothermal lines for the following: dispersed phase flow rate, temperature difference, continuous phase column height, initial dispersed drops diameter, sodium chloride content in water and dispersed phase substance. These figures represent the behavior of temperature distribution during the later stages of simulation. During the early stages the temperature distribution is almost uniform and the heat transfer take place by conduction and convection. However, as the simulation proceeds, the convective and heat sink effect increased in magnitude and isothermal lines become closer to the distribution and symmetry. It is clear that the temperature gradient increased rapidly in the vicinity of column wall and lower column portion, but it increased slightly at the column core and upper column portion.

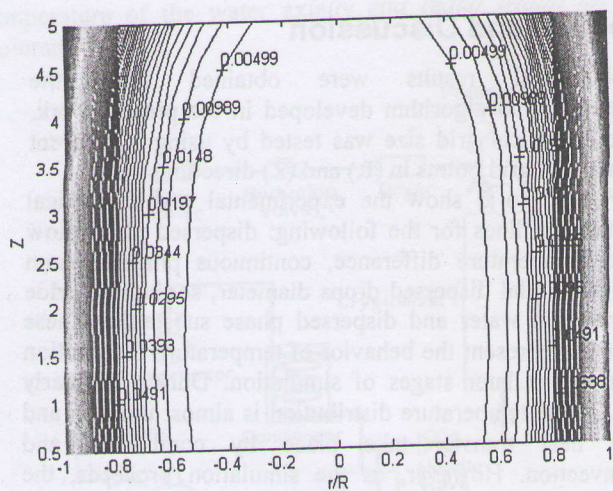
Also Figs. 1 to 6 show the dimensionless temperature contours plotted in (R - Z) plane, and for the systems and parameters studied. These figures show that the center of contour lines lie on the center of the computational domain. At sections near the distributor, the values of contours lines are lower than that section far from it. This means that the temperature increases continuously with moving upward due to the decreasing effect of convective and heat sink.

It was found that the heat sink term has a greatest effect on the temperature distribution, while the dissipation term has a lowest effect on the temperature distribution.

The temperature variation with time was found, influenced greatly with changing the initial drop diameters and dispersed phase flow rate. But it was influenced slightly with changing the temperature difference and continuous phase height.



(a)



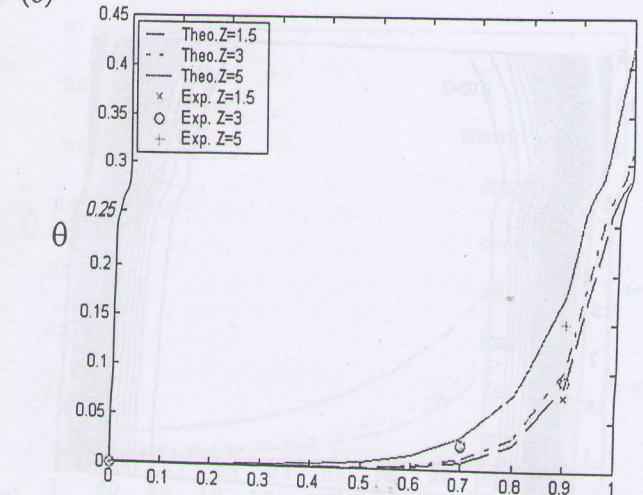
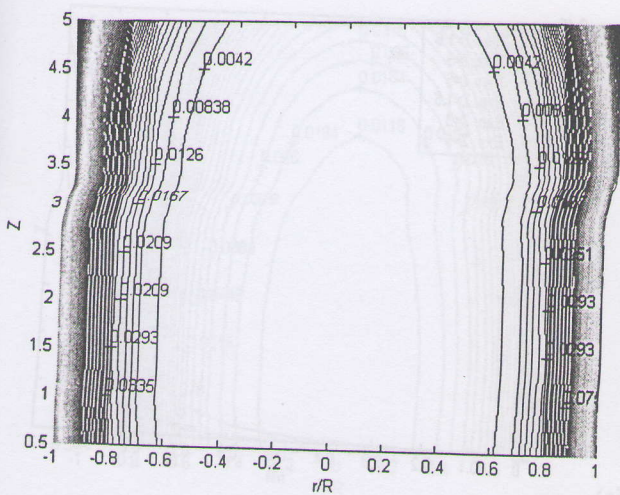
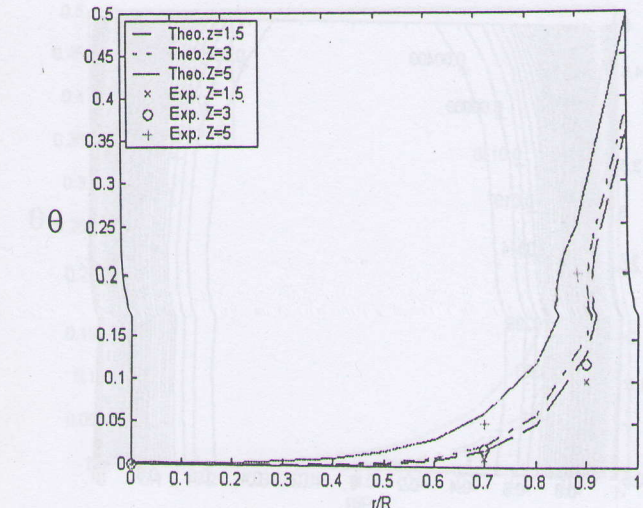
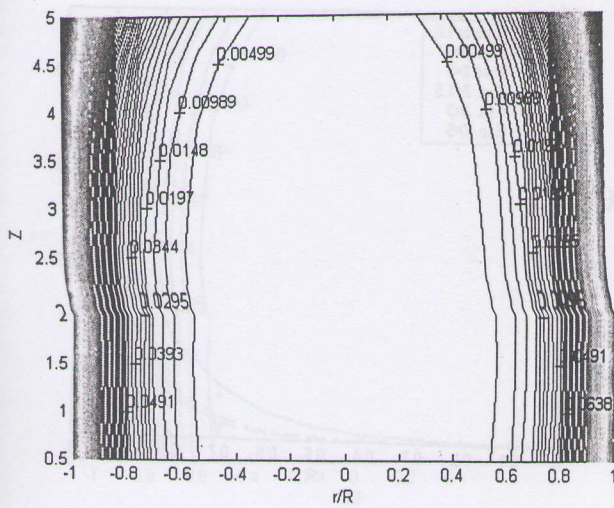
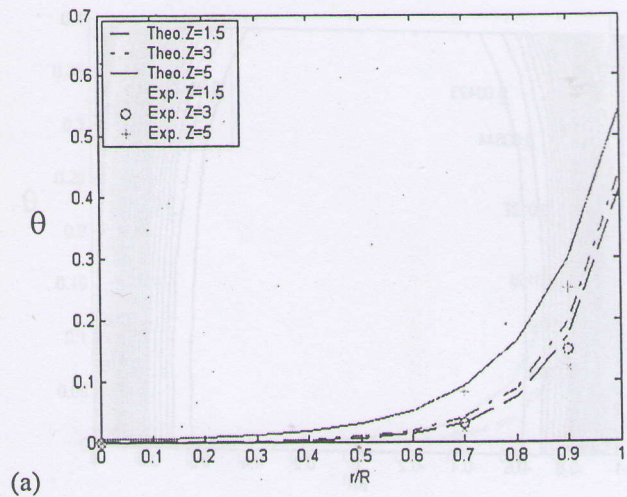
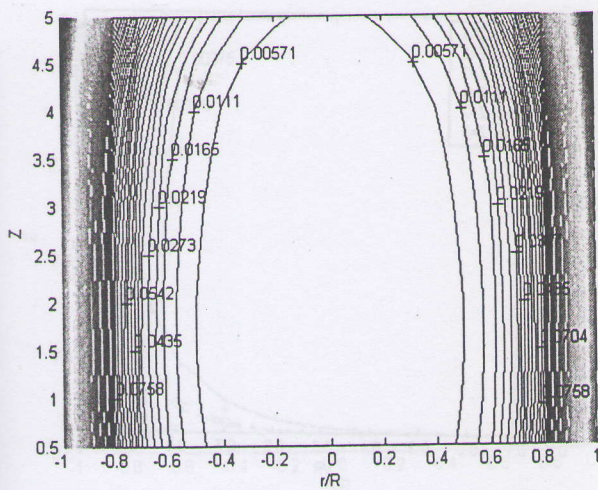
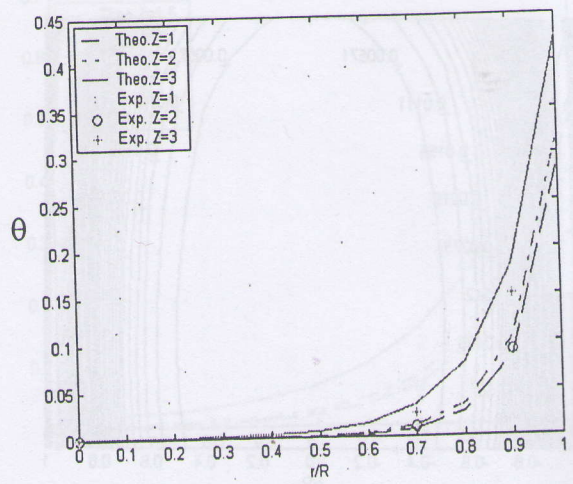
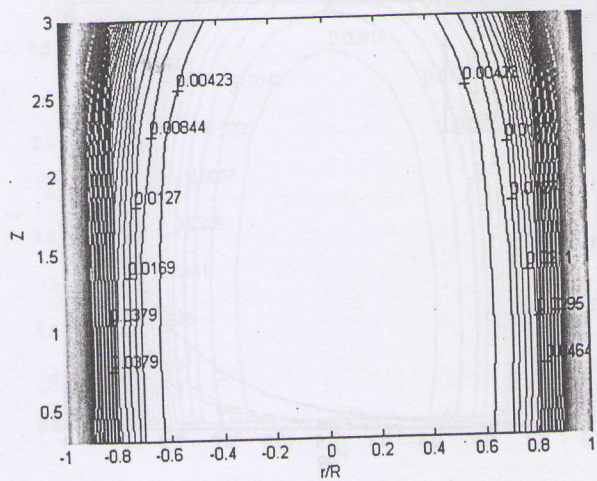
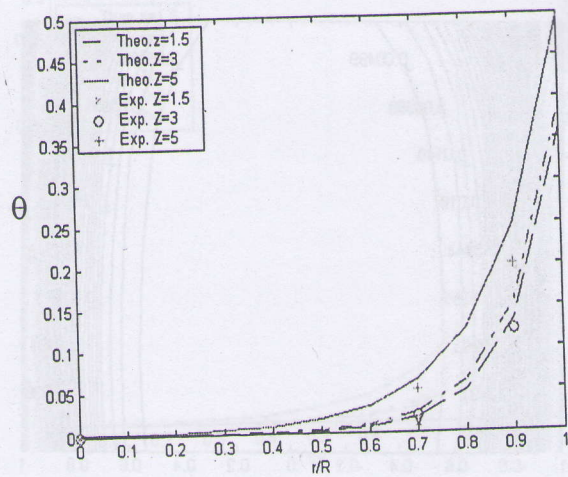
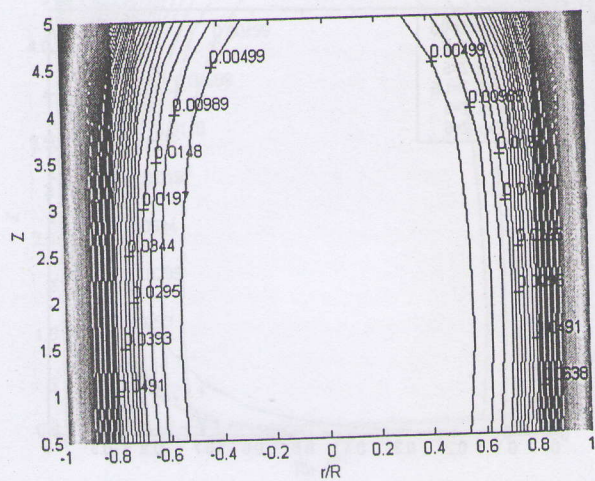


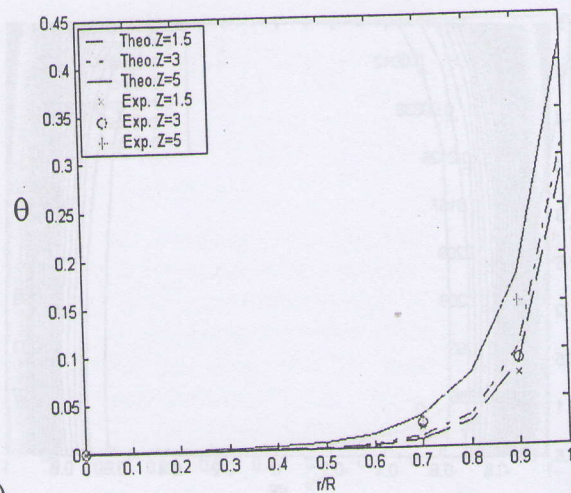
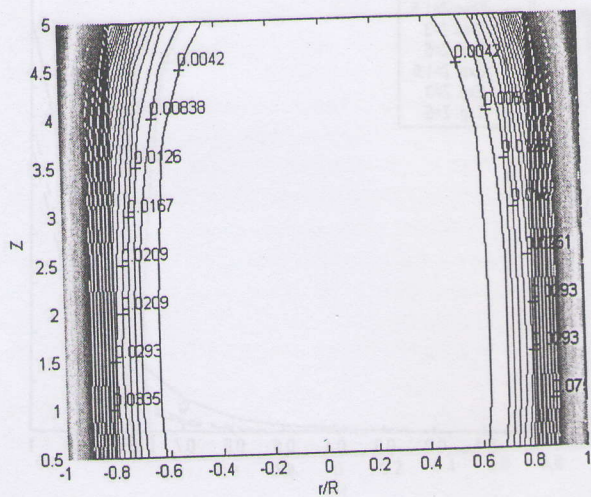
Fig. 4 Temperature distribution for R12 in water with different temperature difference (a) 8°K (b) 5°K (c) 3°K



(a)

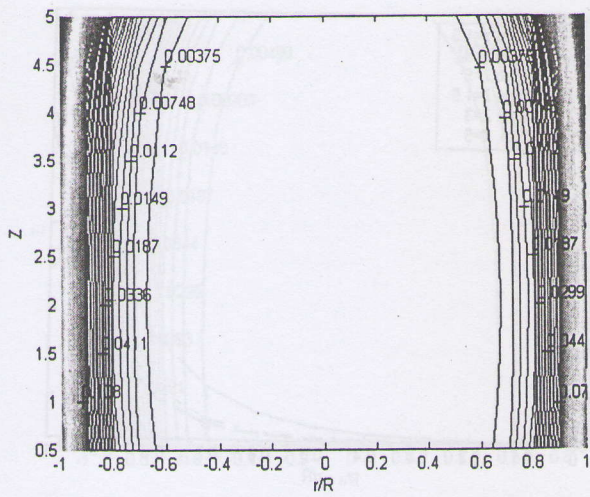


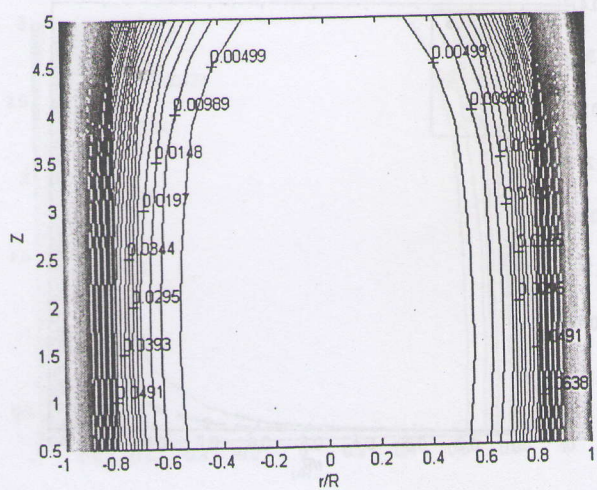
(b)

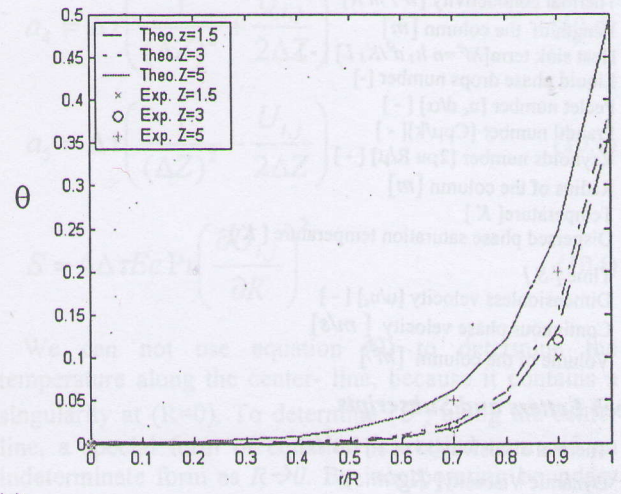
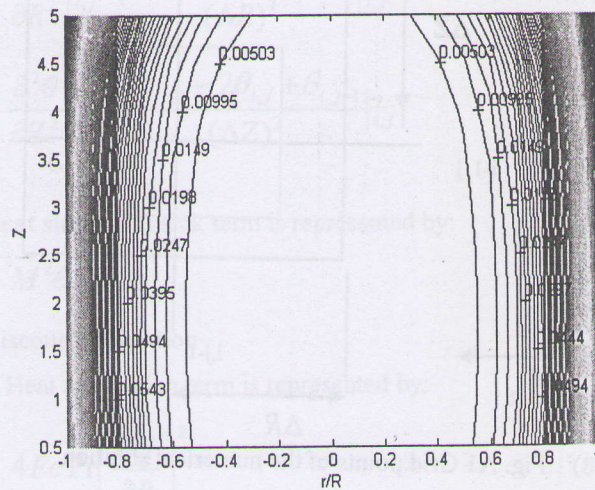
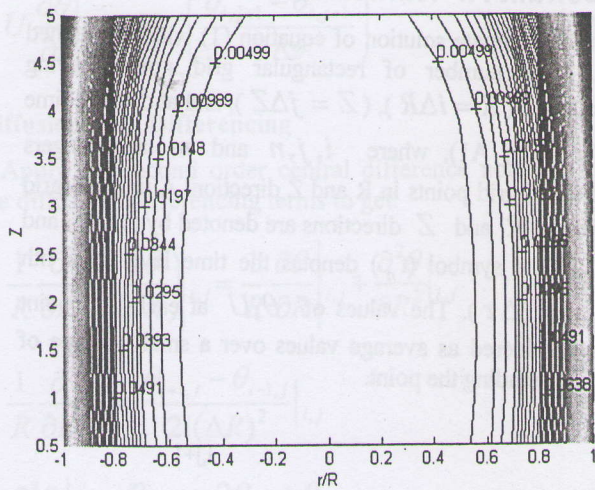


(c)

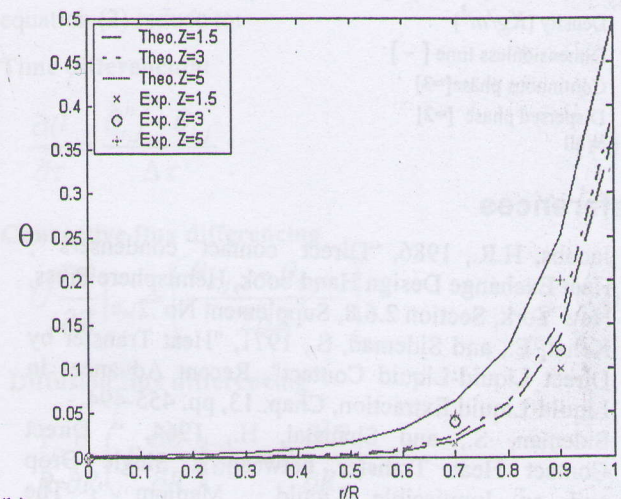
Fig. 5 Temperature distribution for R12 in water with different column height (a) 0.25 m (b) 0.4 m (c) 0.5 m







(a)



(b)

Fig. 8 Temperature distribution for R12 and R134a in water with different dispersed phase substance (a) R12 (b) R134a

Conclusions

There was an acceptable agreement between the experimental and the theoretical results regarding the temperature distribution. The temperature distribution is almost uniform during the early stages of simulation and as the simulation proceeds, the heat transfer take place by conduction and convection leading to increase the convective and heat sink effect in magnitude and isothermal lines become closer to the distribution and symmetry. The center of contour lines lie on the center of the computational domain. At sections near the distributor, the values of contours lines are lower than that section far from it. This means that the temperature increases continuously with moving upward due to the decreasing effect of convective and heat sink.

It was found that the heat sink term has a greatest effect on the temperature distribution, while the dissipation term has a lowest effect on the temperature distribution. The temperature variation with time was found, influenced greatly with changing the initial drop diameters and dispersed phase flow rate. But it was influenced slightly with changing the temperature difference and continuous phase height.

Nomenclature

- C_p Specific heat at constant pressure [J/kg K]
- A_d Instantaneous area of the two-phase bubble [m²]
- d Equivalent diameter of the two-phase bubble [m]
- D_o Diameter of the column [m]
- E_c Eckert Number [$u_c^2/C_{p3}(T_w-T_d)$] [-]
- H Instantaneous heat transfer coefficient [W/m^2K]

- K Thermal conductivity [W/mK]
- L Length of the column [m]
- M^2 Heat sink term [$M^2 = n h_3 d^2 / K_3 L$] [-]
- n Liquid phase drops number [-]
- Pe Peclet number [$u_c d / \alpha$] [-]
- Pr Prandtl number [$C_p \mu / k$] [-]
- Re Reynolds number [$2 \rho u R / \mu$] [-]
- R_0 Radius of the column [m]
- T Temperature [K]
- T_d Dispersed phase saturation temperature [K]
- t Time [s]
- U Dimensionless velocity [u / u_c] [-]
- u_c Continuous phase velocity [m/s]
- V_d Volume of the column [m^3]

Greek Letters and Subscripts

- α Thermal diffusivity [$k / \rho C_p$] [m^2/s]
- μ Dynamic Viscosity [$Kg/m.s$]
- ν Kinematics Viscosity [m^2/s]
- ρ Density [Kg/m^3]
- τ Dimensionless time [-]
- C Continuous phase [=3]
- d Dispersed phase [=2]
- W Wall

References

1. Jacobs, H.R., 1986, "Direct contact condensers", Heat Exchange Design Hand book, Hemisphere Press, New York, Section 2.6.8, Supplement No .2 .
2. Kehat, E., and Sideman, S., 1971, "Heat Transfer by Direct Liquid-Liquid Contact", Recent Advances in Liquid-Liquid Extraction, Chap. 13, pp. 455-494.
3. Sideman, S., and Shabatai, H., 1964, " Direct Contact Heat Transfer between a Single Drop and an Immiscible Liquid Medium ", The Canadian Journal of Chemical Engineering, Vol.42, pp. 107-117.
4. Mori, T., and Mori, Y. H., 1989, "Characterization of gas hydrate formation in direct -contact Cool storage process", Int. J. Refrigeration., Vol. 12, pp.259-265.
5. Jenson, V.G., and Jeffrey, G.V., 1977, "Mathematical Methods in Chemical Engineering", Academic Press, Inc.
6. Gerald, C.F., and Wheatley, P.O., 1985, "Applied Numerical Analysis", Addison-Welsey Publishing Co.
7. Turner, P. R., 1989, "Guide to Numerical Analysis", Macmilland Education LTD.
8. Walter, J.F, and Blanch, H. W., 1983, "Liquid Circulation Patterns and Their Effect on Gas Hold-up and Axial Mixing in Bubble Columns" Chem. Eng. Comm. Vol. 19 , pp.243-262.
9. Sideman, and Isenberg, 1967, " Direct Contact Heat Transfer With Bubble Growth in Three Phase System, Desalination", Vol.2, pp.207-214.

Appendix A: 'Numerical Formulation'

An approximate solution of equation (1) will be obtained at a finite number of rectangular grid points having coordinates: ($R = i\Delta R$), ($Z = j\Delta Z$), and at discrete time t_n (see Fig. A1), where i, j, n and m are integers numbers of grid points in R and Z direction. A uniform grid spacing in R and Z directions are denoted by (ΔR) and (ΔZ). The symbol (t_n) denotes the time level after nth time step ($\Delta \tau$). The values of θ, U at each grid point were considered as average values over a small volume of fluid surrounding the point.

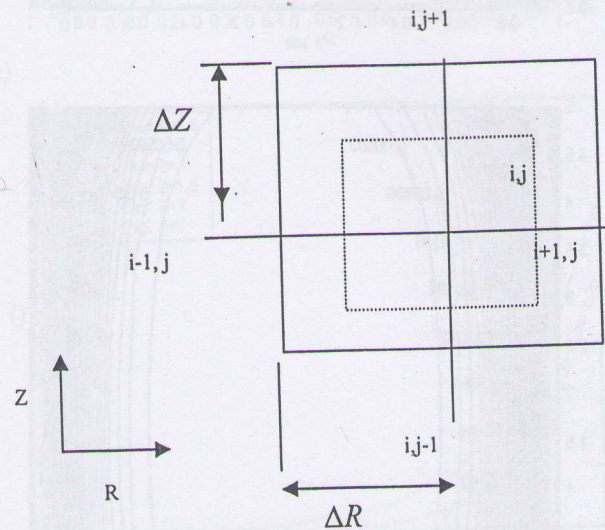


Fig. A1 Grid points of the numerical solution

To solve the energy equation numerically by applying the explicit finite difference method, the derivatives in this equation could be replaced by the following finite difference approximations [5-7].

Time differencing

Apply the first order forward finite difference notation method to the time differencing term to get:

$$\frac{\partial \theta}{\partial \tau} = \frac{\theta_{i,j}^n - \theta_{i,j}}{\Delta \tau} \quad (1)$$

where $\theta_{i,j}^n$ represents the temperature at time ($\tau + \Delta \tau$), and $\theta_{i,j}$, the temperature at time, τ .

Convective flux differencing

Apply first order forward difference notation to the convective flux differencing term to get:

$$U \frac{\partial \theta}{\partial z} \Big|_{i,j} = U_{i,j} \left(\frac{\theta_{i,j+1} - \theta_{i,j-1}}{2\Delta z} \right) \quad (2)$$

Diffusion Flux Differencing

Apply the second order central difference notation to the diffusions differencing terms to get:

$$\frac{1}{R} \frac{\partial}{\partial R} \left(R \frac{\partial \theta}{\partial R} \right) \Big|_{i,j} = \frac{1}{R} \frac{\partial \theta}{\partial R} \Big|_{i,j} + \frac{\partial^2 \theta}{\partial R^2} \Big|_{i,j} \quad (3)$$

$$\frac{1}{R} \frac{\partial}{\partial R} \Big|_{i,j} = \frac{\theta_{i+1,j} - \theta_{i-1,j}}{2i(\Delta R)^2} \Big|_{i,j} \quad (4)$$

$$\frac{\partial^2 \theta}{\partial R^2} \Big|_{i,j} = \frac{\theta_{i+1,j} - 2\theta_{i,j} + \theta_{i-1,j}}{(\Delta R)^2} \Big|_{i,j} \quad (5)$$

$$\frac{\partial^2 \theta}{\partial Z^2} \Big|_{i,j} = \frac{\theta_{i,j+1} - 2\theta_{i,j} + \theta_{i,j-1}}{(\Delta Z)^2} \Big|_{i,j} \quad (6)$$

Heat sink. Heat sink term is represented by:

$$M^2 \theta_{i,j} \quad (7)$$

Viscous dissipation

Heat dissipation term is represented by:

$$4EcPr \left(\frac{\partial U}{\partial R} \right)^2 \quad (8)$$

substituting equations (1), to (8) into the dimensionless governing energy equation, we obtain:

$$\theta_{i,j}'' = a_1 \theta_{i-1,j} + a_2 \theta_{i+1,j} + a_3 \theta_{i,j} + a_4 \theta_{i,j-1} + a_5 \theta_{i,j+1} + S \quad (9)$$

where the a_k , denote coefficients which vary in time but which are constant over a time step.

$$a_1 = 4\Delta\tau \left(\frac{i-0.5}{i(\Delta R)^2} \right) \quad (10.a)$$

$$a_2 = 4\Delta\tau \left(\frac{i+0.5}{i(\Delta R)^2} \right) \quad (10.b)$$

$$a_3 = 1 - \Delta\tau \left(\frac{8}{(\Delta R)^2} + \frac{2}{(\Delta Z)^2} + M^2 \right) \quad (10.c)$$

$$a_4 = \Delta\tau \left(\frac{1}{(\Delta Z)^2} + \frac{U_{i,j}}{2\Delta Z} \right) \quad (10.d)$$

$$a_5 = \Delta\tau \left(\frac{1}{(\Delta Z)^2} - \frac{U_{i,j}}{2\Delta Z} \right) \quad (10.e)$$

$$S = 4\Delta\tau EcPr \left(\frac{\partial U_{i,j}}{\partial R} \right)^2 \quad (10.f)$$

We can not use equation (9) to determine the temperature along the center-line, because it contains a singularity at (R=0). To determine (θ) along the center line, a special form of equation is needed to avoid an indeterminate form as $R \rightarrow 0$. By incorporating boundary condition at (R=0) and using L'Hospital's rule, equation (2) reduce to:

Time differencing:

$$\frac{\partial \theta}{\partial \tau} = \frac{\theta_{i,j}^n - \theta_{i,j}}{\Delta\tau} \quad (11)$$

Convective flux differencing

$$U \frac{\partial \theta}{\partial Z} \Big|_{0,j} = \left(\frac{\theta_{o,j+1} - \theta_{o,j-1}}{2\Delta Z} \right) \quad (12)$$

Diffusion flux differencing

$$\begin{aligned} \frac{1}{R} \frac{\partial}{\partial R} \left(R \frac{\partial \theta}{\partial R} \right) \Big|_{o,j} &= 2 \frac{\partial^2 \theta}{\partial R^2} \Big|_{o,j} \\ &= 2 \left(\frac{\theta_{i,j} - 2\theta_{o,j} + \theta_{-1,j}}{(\Delta R)^2} \right) \end{aligned} \quad (13)$$

$$(\theta_{-1,j}) = (\theta_{1,j}) \text{ due to symmetry} \quad (14)$$

$$\frac{1}{R} \frac{\partial}{\partial R} \left(R \frac{\partial \theta}{\partial R} \right) \Big|_{o,j} = 4 \frac{(\theta_{1,j} - \theta_{0.5})}{(\Delta R)^2} \quad (15)$$

$$\frac{\partial^2 \theta}{\partial Z^2} \Big|_{o,j} = \frac{\theta_{o,j+1} - 2\theta_{o,j-1}}{(\Delta Z)^2} \quad (16)$$

Heat sink

$$M^2 \theta_{o,j} \quad (17)$$

Viscous Dissipation

$$4EcPr \left(\frac{\partial U}{\partial R} \right)^2 \Big|_{o,j} = 0 \text{ due to } U_{o,j} = 1 \quad (18)$$

Substituting equations (11), to (18) into the dimensionless governing energy equation, we obtain:

$$\theta_{o,j}'' = b_1 \theta_{1,j} + b_2 \theta_{o,j} + b_3 \theta_{o,j-1} + b_4 \theta_{o,j+1} \quad (19)$$

where the b_k denote coefficient which vary in time but which are constant over a time step.

$$b_1 = \Delta\tau \left(\frac{16}{(\Delta R)^2} \right) \quad (20.1)$$

$$b_2 = 1 - \Delta\tau \left(\frac{16}{(\Delta R)^2} + \frac{2}{(\Delta Z)^2} + M^2 \right) \quad (20.2)$$

$$b_3 = \Delta\tau \left(\frac{1}{(\Delta Z)^2} + \frac{1}{2\Delta Z} \right) \quad (20.3)$$

$$b_4 = \Delta\tau \left(\frac{1}{(\Delta Z)^2} - \frac{1}{2\Delta Z} \right) \quad (20.4)$$